Desalination and Water Treatment
www.deswater.com
doi: 10.1080/19443994.2013.801322

52 (2014) 3403–3410
April

Taylor & Francis
Taylor & Francis Group

Enhancing decolorization of Eriochrome Blue Black R during nano-size zero-valent iron treatment using ultrasonic irradiation

Shokooh Sadat Khaloo[a,*], Shokoufeh Fattahi[b]

[a]*Faculty of Health, Safety and Environment, Department of Science, Shahid Beheshti University of Medical Sciences, P.O. Box 16858-116, Tehran, Iran*
Tel. +98 21 77309961 65; Fax: +98 21 77302969; email: sh_khaloo@sbmu.ac.ir
[b]*Faculty of Health, Safety and Environment, Department of Hygiene Sciences, Shahid Beheshti University of Medical Sciences, P.O. Box 16858-116, Tehran, Iran*

Received 14 November 2012; Accepted 23 April 2013

ABSTRACT

The effectiveness of nano-size zero-valent iron (NZVI) particles for treatment of Eriochrome Blue Black R (EBBR), a representative azo dye, under ultrasonic irradiation was determined. The influence of experimental variables such as, initial solution pH, NZVI dosage, irradiation time, initial dye, NaCl, and Na_2CO_3 concentrations on removal efficiency of color were investigated. It was found that the kinetic rate constant of sonocatalytic destruction of EBBR in presence of NZVI was significantly enhanced under acidic conditions. The degradation rate constants of dye increased by increasing of NZVI dose and irradiation time, but decreased by increasing the initial dye concentration. Although, increasing NaCl concentration from 0.1 to 1% (w/v) improved the kinetic removal rate from 0.16 to 0.29 min^{-1} but, presence of Na_2CO_3 had no significant effect on the degradation rate. The UV–vis spectrum showed that complete decolorization of synthetic solutions contain 100 ppm EBBR by 0.3 g/L NZVI at initial pH solution 3, occurred at 20 min ultrasonic irradiation.

Keywords: Decolorization; Nano-size zero-valent iron; Eriochrome Blue Black R (EBBR)

---

1. Introduction

Azo dyes are synthetic organic dyes contain the azo chromophoric group (-N=N-). This divalent group is attached to sp^2 hybridized carbon atoms on one side, to an aromatic or heterocyclic nucleus on the other; it may be linked to an unsaturated molecule of the carboxylic, heterocyclic, or aliphatic type. No natural dyes contain this chromophore. Commercially, the azo dyes are the largest and most versatile class of organic dyestuffs. There are more than 10,000 Color Index generic names assigned to commercial colorants, approximately 4,500 are in use and over 50% of these belong to the azo class [1]. Azo dyes are used in large quantities in several industries such as textile, paper, inks, leather, drug, and food processing. The effluents from these industries contain dyes and organic pollutants. Most of these dyes are carcinogenic, harmful, and reduce the light penetration in aqueous systems, therefore causing a disturbance in the natural growth activity of aquatic life. On the other hand, some of these dyes pass into drinking water and can cause damage to human life. Therefore, it is essential to remove these dyes from water or treat them in such a way to minimize the damage to the environment. Azo dyes resist aerobic and short-time

---

*Corresponding author.

anaerobic treatment [2] and under anaerobic conditions azo dyes are cleaved by micro-organisms, forming potentially carcinogenic aromatic amines such as alkylated derivatives of aniline, naphthylamine derivatives, and benzidine derivatives [2]. This creates an urgent demand for the development of multistep treatment concepts which guarantee not only irreversible decolorization but also mineralization of azo dyes.

There is, currently a wide range of treatment technologies for these types of wastewater. Physical methods (adsorption [3], ion exchange [4], chemical methods, electrochemical degradation [5,6], ozonation [7,8], and biological degradation [9,10]) are typical methods that have own advantages and disadvantages. The main disadvantages of these methods are incomplete ion removal, high energy requirements, low efficiency, and production of toxic sludge or other toxic waste product that require further disposal or treatment.

In recent years, a great deal of attention has been paid to develop new treatment strategies for degradation of dye molecules. Zero-valent iron (ZVI) is a strong reducing agent and can donate two electrons to many environmental contaminants hence, ZVI particles have been studied for the treatment of wastewater contaminated with chlorinated organic compound [11,12], heavy metal ions [13,14], nitrate [15,16] and, dyes [17–19]. To enhance the reduction effect of ZVI particles, some strategies have been applied such as coating iron particles with a second catalytic metal [16], modification with surfactant [20], and reducing particles size down to nanometer [21]. The kinetic of reactions with ZVI in batch experiments appears to be influenced by mass transport of the oxidant to the metal surface [21]. The large surface area and high surface reactivity of nanoparticles can enhance the kinetic rate of the reaction. Nano-zero-valent iron (NZVI technology) represents one of the pseudo-first generations of nanoscale environmental clean-up technologies.

Sonochemistry arises from acoustic cavitations: the formation, growth, and implosive collapse of bubbles in a liquid due to irradiation with high intensity sound or ultrasound radiations. The collapses of bubbles produce locally high pressure and temperature peaks, which results in a number of pyrolytic reactions [22]. Ultrasonication of azobenzene and related azo dyes is said to lead to production of high toxic nitrosoaromatics [23]. Therefore, it is of outstanding interest to find a combination with another treatment to enhance dye degradation and avoiding toxic degradation products. The scope of the present study is treating EBBR in aqueous solution using NZVI particles. The synergetic effect of ultrasonic radiation on the removal efficiency of EBBR in presence of NZVI particles was investigated. NZVI particles were synthesized by wet reduction method and were characterized using electron scanning microscopy (SEM) and X-ray diffraction (XRD) methods.

2. Experimental procedures

2.1. Materials

Eriochrome Blue Black R (EBBR) was purchased from Fluka. Ferrous sulfate ($FeSO_4.7H_2O$), sodium borohydride ($NaBH_4$, 96%), hydrochloric acid (HCl), and Sodium hydroxide (NaOH) were purchased from Merck (Darmstadt, Germany). The chemical structure of dye is illustrated in Table 1. Double distilled water was used to prepare all solutions. Stock solutions of 0.01 M azo dye was prepared and other working solutions were obtained by successive dilution of stock solutions.

2.2. Preparation of NZVI

The NZVI particles were synthesized by the well-known wet reduction method [24]. Reagents were prepared using deoxygenated double-distilled water with N_2 gas for 30 min. About 50 ml 0.4 M sodium borohydride solution (0.8075 g $NaBH_4$) was dropped into the 100 ml 0.1 M $FeSO_4.7H_2O$ (2.8111 g $FeSO_4.7H_2O$) under

Table 1
The characteristics of Eriochrome Blue Black R (EBBR)

Azo dye	Formula	MW	λ_{max}	Solubility in water
Eriochrome Blue Black R	$C_{20}H_{13}N_2O_5Na$	416.4	530 nm	20 mg/mL
Chemical structure	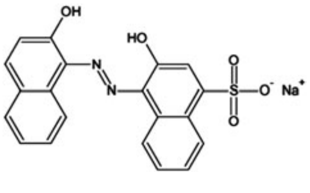	$pK_{a(solfunic\ group)}= 1$ $pK_{a2} = 7.4$ $pK_{a3} = 13.8$		

vigorous mixing for 20 min on a shaker. Ferrous ion was reduced to elemental iron by borohydride according to the following equation:

$$Fe^{2+}_{(aq)} + 2BH_4^- + 6H_2O \rightarrow Fe^0_{(s)} + 7H_{2(g)} + 2B(OH)_{3(aq)} \quad (1)$$

The solution was centrifuged at 3,400 rpm for 5 min and washed three times with 10 ml of deoxygenated double-distilled water to remove the residual reagents. The wet paste was suspended in 10^{-4} M deoxygenated hydrochloric acid. The size and shape of the NZVI particles were determined using a SEM.

2.3. Batch decolorization experiments

Batch experiments were conducted to evaluate the effect of the initial pH, irradiation time, NZVI dose, and initial dye concentration on the destruction efficiency of dye by NZVI particles. The pH of dye solutions (100 ppm) was adjusted to the desired levels from 2.5 to 8.5 using HCl (0.5 M) and NaOH (0.5 M). The dye solution was bubbled with air for 10 min before experiments. About 50 ml of dye solution was transferred into a beaker and placed in an ultrasonic apparatus (Elmasonic E 60 H, 37 kHz 400 W, continuous wave mode, Germany). Various amounts of NZVI suspension were added to the beaker to yield final iron concentrations of 0.1, 0.2, 0.3, and 0.4 g/L. At preselected time intervals, samples were withdrawn and centrifuged at 3,500 rpm for 5 min, and the supernatant was analyzed using UV–vis spectrophotometer (AvaSpec-2048, Avantes, the Netherlands). Following the absorbance between 200 and 700 nm provided qualitative information related to the degradation of azo bond and aromaticity of the dye during sonolysis. In addition, decolorization efficiency was followed quantitatively by measuring the decreases in absorbance of dye chromophore at $\lambda_{\max}$ 530 nm. Each experiment was performed four times and the standard deviation of the experiments was calculated.

COD was determined by the open reflux method [25]. Percentage COD remaining was calculated by the following equation:

$$\%\ \text{COD remaining} = (\text{final COD}/\text{initial COD}) \times 100 \quad (2)$$

3. Results and discussion

3.1. Characterization of NZVI

The NZVI particles were characterized by SEM and XRD. Fig. 1(A) shows SEM image of synthesized NZVI particles (SEM, KYKY-EM3200, China). As you can seen the synthesized NZVI particles are almost spherical with diameters lower than 100 nm. Some of these spherical nanoparticles aggregated together to form rod structures due to magnetic interaction and the natural tendency to remain in a more thermodynamically stable state. The X-ray diffraction pattern of NZVI is shown in Fig. 1(B). X-ray powder diffraction of NZVI particles have been obtained by a D8 Advanced Bruker diffractometer. The spectrum shows a major diffraction intensity peak at $2\theta = 47^\circ$. The characteristic diffraction peaks of iron oxides or hydroxides were not detected. This indicated that the iron present in the sample is mainly in zero-valent state, and all zero-valent iron is in single-phase α-Fe^0.

3.2. Sonolysis

The typical UV–vis spectrum of EBBR was shown in Fig. 2(a). Absorbance band at 274 nm (attributed to $\pi \rightarrow \pi^*$ transition in aromatic ring) represents aromatic character of the dye. The band at 530 nm (attributed to $n \rightarrow \pi^*$ transitions of N=N, C=N, C=O chromophore groups) is responsible for the color of the dye solution and is thus used to monitor the rate of decolorization of the dye. Therefore, decreases in absorbance at 274 and 530 nm correspond to loss of aromaticity and cleavage of azo bond of the dye during degradation [26]. NZVI assisted sonochemical degradation was carried out and the results are shown in Fig. 2(d) after 6 min of reaction. In contrast, the absorption peaks in the presence of NZVI without ultrasonic irradiation (on a shaker, Fig. 2(c)) and under ultrasonic irradiation in the absence of NZVI (Fig. 2(b)) were little changed and almost unchanged, respectively. The results indicate that the combination of NZVI and ultrasound irradiation (Fig. 2(d)) have synergetic effect on degradation of dye.

The removal efficiency respect to time of exposure to ultrasound irradiation was investigated. The results show clearly that the degradation efficiency of dye increases with an increase in irradiation time and more than 96% of degradation was achieved in 20 min. The degradation of dye on NZVI surface is attributed to the reduction of O_2 on Fe^0 lead to in situ production of H_2O_2 and Fe^{2+} that is responsible for the $^\cdot OH$ radical induced oxidation occurring on metallic iron surface (reaction 3, 4) [27].

$$Fe^0 + O_2 + 2H^+ \rightarrow Fe^{2+} + H_2O_2 \quad (3)$$

$$Fe^{2+} + H_2O_2 \rightarrow Fe^{3+} + HO^\cdot + HO^- \quad (4)$$

The enhancement in the $^\cdot OH$ radical formation rate can increase the efficiency of the degradation. In this

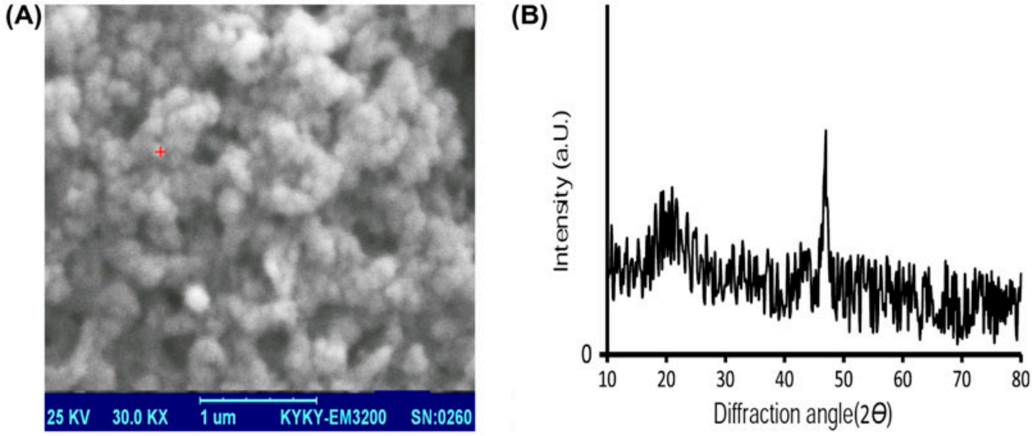

Fig. 1. (A) SEM image and (B) X-ray diffraction patterns of the synthesized NZVI particles.

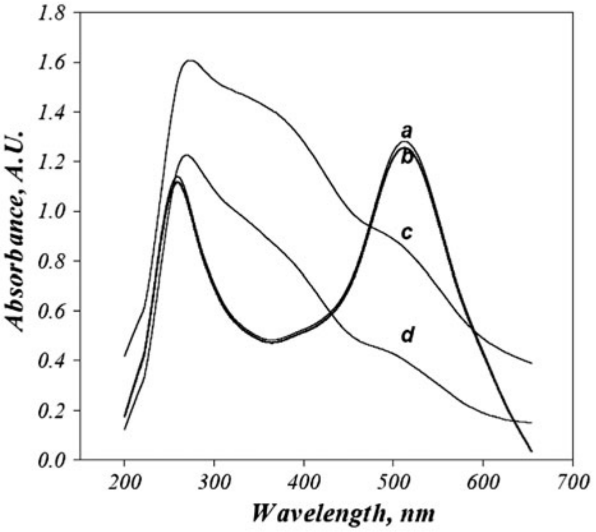

Fig. 2. UV–vis spectrum of 100 ppm EBBR at pH 3 and different conditions: (a) mother solution, (b) after 6 min sonication in absence of NZVI, (c) after 6 min shaked in presence of 0.3 g/l NZVI, (d) after 6 min sonication in present of 0.3 g/l NZVI.

respect, ultrasound irradiation may enhance the generation of oxidative species in water by the hemolytic cleavage of water molecules by pyrolitic reactions, which may be presented as follows:

$$H_2O \rightarrow HO^{\cdot} + H^{\cdot} \qquad (5)$$

$$2HO^{\cdot} + 2H^{\cdot} \rightarrow H_2O_2 + H_2 \qquad (6)$$

The $^{\cdot}OH$ radical and H_2O_2 are strong oxidizing agents, which are responsible for the degradation of organic substances [28].

3.3. Influence of initial pH on the sonocatalytic degradation of EBBR

The effect of initial pH on the sonochemical decomposition of dye was investigated in the range 2.5–8.5. It is obvious that the λ_{max} of EBBR change (from 520 to 610 nm) with increasing of medium pH from 2.5 to 8.5. Then the degradation percent of color at different pH was determined according to the reduction of absorbance band at corresponding λ_{max} to each pH. The results (Fig. 3) indicate that the catalytic activity of NZVI combined ultrasound radiation increases with the decrease of initial pH from 8.5 to 2.5. More detailed information about the effect of solution pH is demonstrated by studying the kinetics of the degradation reaction. The inset of Fig. 3 shows the pseudo-first-order kinetic model fit for the degradation of EBBR under various initial pH conditions

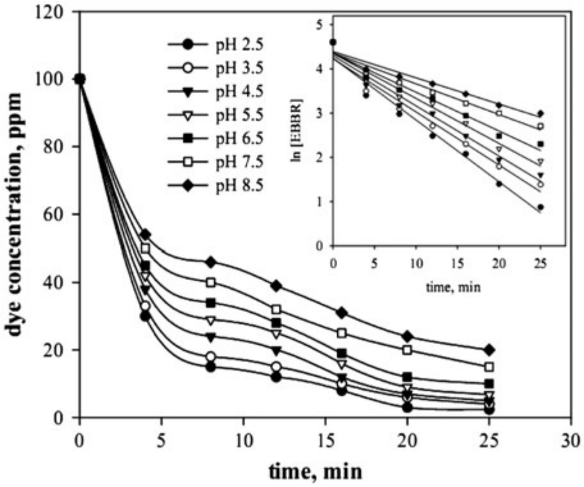

Fig. 3. Effect of initial pH on degradation of 100 ppm EBBR,in presence of 0.3 g/l NZVI. Inset: the logarithm of the dye concentration vs. time at various pH.

Table 2
Statistical results for comparison of pseudo-first-order rate constants at various initial pH levels ($F_{\text{tab}(0.05),3,3} = 9.28$ and one way $t_{\text{tab}(0.05),6} = 1.94$)

No.	pH	k, min^{-1a}	F_{exp}^{b}	S_{pooled}^{c}	$t_{\text{exp.}}$	r^2
1	2.5	0.141 ± 0.0062	–	–	–	0.9723
2	3.5	0.132 ± 0.0068	0.58	0.0070	2.02	0.9624
3	4.5	0.115 ± 0.0057	1.42	0.0072	3.11	0.9658
4	5.5	0.100 ± 0.0056	1.04	0.0065	3.24	0.9660
5	6.5	0.0887 ± .0,051	1.20	0.0062	2.57	0.9600
6	7.5	0.0701 ± 0.0034	2.25	0.0050	5.21	0.9519
7	8.5	0.0598 ± 0.0028	1.47	0.0036	4.07	0.9490

[a] Average of slope ± standard deviation.

[b] F_{exp}1, 2, F_{exp}2, 3, F_{exp}3, 4, F_{exp}4, 5, F_{exp}5, 6, F_{exp}6, 7 have been calculated, respectively.

[c] S_{pooled} 1,2, S_{pooled} 2,3, S_{pooled} 3,4, S_{pooled} 4,5, S_{pooled} 5,6, S_{pooled} 6,7 have been calculated, respectively.

(error bars haven't been shown in Fig. 3 but the statistical results have been summarized in Table 2). Table 2 summarizes the statistical results for comparison of pseudo-first-order rate constants and their corresponding regression values at different pH. The F-test showed that precision of measurements is equal, hence, S_{pooled} values were calculated and then t_{exp} was obtained and compared with the theoretical t value with six degrees of freedom and 0.05 p-value of one-way t-table. Statistical analysis showed that there are significant differences between k values obtained at different pH. On the other hand, it is obvious that the pseudo-first-order model fits well with the experimental data. The experimental results reveal that the kinetic of decolorization of EBBR (100 ppm) was very fast in acidic solution (pH 2.5–3.5), but relatively slow in neutral or basic solutions. Similar results was observed and reported while treating other chemicals with NZVI, such as methyl orange and chlorinated ethanes [29,30]. The low pH may remove the passive layers from the NZVI core, rendering them free to react to generate hydroxyl radicals effectively. On the other hands at high pH, the ferrous and ferric ions dissolved from the surface of NZVI according to the Eqs. (3) and (4) are able to collide with hydroxyl ions in the alkaline solution to produce oxides and hydroxides of Fe(III) or Fe(II). These compounds precipitate on the NZVI surface and occupy the reactive sites, hindering the reaction. According to the pKa values of EBBR it is obvious that in the pH range studied the dye apparent as an anion, then at neutral and alkaline pH the color removal might be attributed to the adsorption of deprotonated dye ions onto the iron oxide formed on the NZVI particles [31]. It is speculated that at acidic medium, the decolorization was accomplished by ZVI reduction of dye molecules (Eqs. (3) and (4)). At neutral and alkaline medium decolorization might be attributed to the adsorption of the dye molecules onto the iron oxide formed on the NZVI particles:

$$\text{Fe}^0 + 2\text{H}_2\text{O} \rightarrow \text{Fe(OOH)} + \frac{3}{2}\,\text{H}_2\text{O} \tag{7}$$

$$\text{Fe(OOH)} + \text{D}^{2-} \rightarrow \text{Fe(OOH)D}^{-} \tag{8}$$

where Fe(OOH) represent ferrioxyhydroxide and D^{2-} is the deprotonated dye ions at neutral pH.

3.4. Influence of NZVI concentration on the sonocatalytic degradation of EBBR

The effect of NZVI dosage on the degradation of EBBR is demonstrated in Fig. 4 (error bars haven't been shown in Fig. 4 but the statistical results have

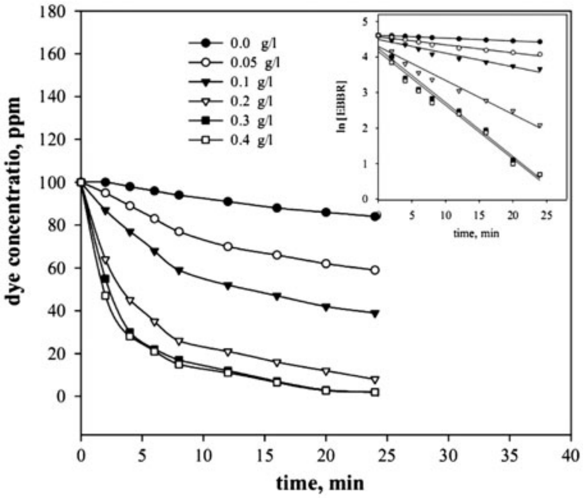

Fig. 4. Effect of NZVI concentration on degradation of 100 ppm EBBR at pH = 3. Inset: the logarithm of the dye concentration vs. time at various NZVI dosages.

Table 3
Statistical results for comparison of pseudo-first-order rate constants at various NZVI concentrations, ($F_{tab(0.05),3,3} = 9.28$ and one way $t_{tab(0.05),6} = 1.94$)

No.	[NZVI], g/l	k, min^{-1a}	$F_{exp}{}^{b}$	$S_{pooled}{}^{c}$	$t_{exp.}$	r^2
1	0.0	0.0079 ± 0.0006	–	–	–	0.9897
2	0.05	0.025 ± 0.0012	4.00	0.0011	21.99	0.9657
3	0.1	0.038 ± 0.0019	2.51	0.0018	9.98	0.9486
4	0.2	0.097 ± 0.0046	5.86	0.0041	20.45	0.9630
5	0.3	0.13 ± 0.0070	2.31	0.0068	6.80	0.9751
6	0.4	0.14 ± 0.0065	0.86	0.0078	1.80	0.9682

[a] Average of slope ± standard deviation.

[b] F_{exp}1, 2, F_{exp}2, 3, F_{exp}3, 4, F_{exp}4, 5, F_{exp}5, 6 have been calculated, respectively.

[c] S_{pooled} 1,2, S_{pooled} 2,3$^{b}S_{pooled}$ 3,4 S_{pooled} 4,5 S_{pooled} 5,6 have been calculated, respectively.

been summarized in Table 3). The degradation efficiency increased by increasing NZVI dose and when NZVI was > 0.3 g/L, almost complete decolorization was achieved after 20 min irradiation. The inset in Fig. 4 shows a logarithmic plot of the EBBR concentration (-Ln[EBBR]) vs. time. The reasonable values of the correlation coefficients (r^2) affirm that the degradation of EBBR by NZVI in presence of ultrasonic radiation follows pseudo-first-order kinetics (Table 3). Statistical analysis showed that there are significant differences between k values obtained at different concentration of NZVI from 0 to 0.3 g/L. At higher concentration of NZVI, k value tended to level off ($t_{exp5,6} < t_{tab}$ in table 3). The rate constant increases linearly with NZVI concentration from 0 to 0.3 g/L ($k = (0.43 \pm 0.01)$ [NZVI] + (0.0040 ± 0.0003), $r^2 = 0.9857$, figure not shown). Thus, the degradation rate constant would increase by 0.43 ± 0.01 min^{-1} per increase of 1 g/L of NZVI concentration. The accelerated reaction rate can be attributed to increase production of $^{\cdot}$OH radicals with increase NZVI dose leading to enhance degradation rate. On the other hand, further increase in NZVI concentration (>0.3 g/L) did not result in increase in the rate of degradation. This phenomenon may be due to the aggregation of nano-sized zero-valent iron particles at high amount, which causes the decrease in the surface active site of NZVI and disturb the transmission of ultrasound in water medium [32].

3.5. Influence of the initial dye, NaCl, and Na_2CO_3 concentration

The effect of the dye concentration on its sonochemical decomposition in presence of 0.3 g/L NZVI was examined. The color removal in various initial dye concentration (50, 100, 200 and 300 ppm) and the pseudo-first-order kinetic plot of degradation at different concentrations of EBBR was shown in Fig. 5 and the corresponding inset, respectively. The results indicate that the removal efficiency of color decreased by increasing dye concentration and a significant decrease in the decolorization rate resulted at high concentration. It is presumably due to saturation of ZVI-reactive surface sites [26] in one side and agglomeration of dye molecules at high concentration in the other [1].

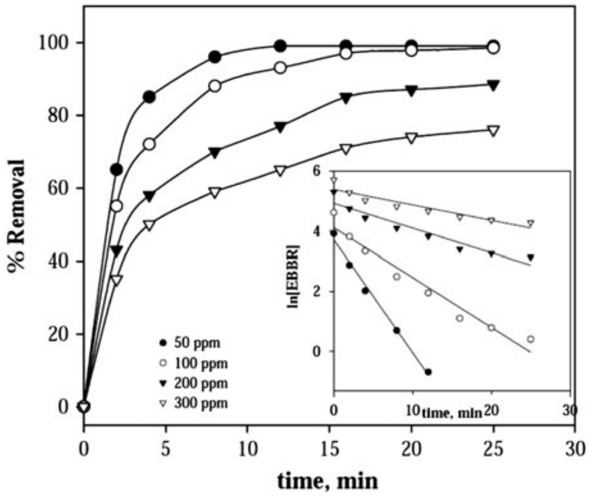

Fig. 5. Effect of the initial dye concentration on degradation of EBBR. Inset: the logarithm of the dye concentration vs. time. Experimental conditions: pH = 3; NZVI = 0.3 g/L.

An additional batch experiments were conducted to study the effect of NaCl and Na_2CO_3 concentration on decolorization of EBBR. The pseudo-first-order kinetic rate constants of degradation of 100 ppm EBBR by 0.3 g/L NZVI under ultrasonic irradiation at pH 2.5 with 0.1, 0.5, and 1% (w/v) of NaCl were 0.16, 0.22, and 0.29 min^{-1}, respectively. The results show that increasing 1% w/v NaCl concentration enhances the removal kinetic rate of EBBR by 0.15 min^{-1}

($k = 0.15[\text{NaCl}] + 0.144$, $r^2 = 0.999$). Previous researches reveal that the addition of chloride increases the degradation rate during NZVI treatment of contaminated water [27,33]. This behavior may be attributed to this fact that chloride salts are known as corrosion promoter [33]. Corrosion the surface of NZVI leads to generate the reactive oxygen species such as $^{\cdot}$OH radicals, which further destruct the azo dye molecules. On the other hand, the addition of salt increases ionic strength of the aqueous phase, which induce an occurrence commonly called the salting-out effect. This phenomenon pushes organic pollutants toward the bubble–bulk solution interface and, therefore, leads to a higher degradation rate [34].

Wastewater is in contact with air and atmospheric CO_2 could dissolve in water easily then, inorganic anions of carbonates occur naturally in wastewater. Carbonate ions could affect the degradation process in different ways (1) scavenging of hydroxyl radicals by carbonate ions reduces the degradation rate of the dye. (2) the presence of ions in solution increases ionic strength of the aqueous phase, which induces salting out effect. (3) presence of inorganic anions lead to decreased electrostatic repulsion between two ionic dye, hence increasing the degree of aggregation of dye which affects their attack by hydroxyl radicals [35]. Different concentrations of Na_2CO_3 from 0.1 to 1 mM were used to study the influence of carbonate ions on the degradation of EBBR. The results show that the presence of carbonate ions has no significant effect on degradation rate of the dye. Since, the experiments were performed in acidic condition most of carbonate ions were presented as H_2CO_3. This neutral molecule did not show any effect, not retardant not accelerator, on degradation of EBBR.

3.6. Mineralization of EBBR

As discussed previously, decrease the absorption band at around 530 nm (in experimental condition, pH=3) is used to follow the rate of decolorization of the dye while decreases in absorbance band at 274 nm indicate the degradation of the aromatic segment of the dye [26]. A decrease in the intensities of the band at 530 and 274 nm suggest that both the chromophore and the aromatic part of the dye were breaking down. Chemical oxygen demand (COD) test is used to measure the amount of organic compounds in water. Decreasing COD is evidence for the oxidation of organic compounds and decrease in the carbon content in the sample, hence indicative of the extent of mineralization. Fig 6 shows the extent of degradation of EBBR by measuring the decrease in COD values due to the treatment of dye solution by NZVI in presence of ultrasonic waves. The results indicate that sonochemical decomposition resulted in 14% mineralization of the dye in 25 min; while NZVI assisted sonochemical degradation was more efficient leading to 89%, mineralization of the dye over the same time.

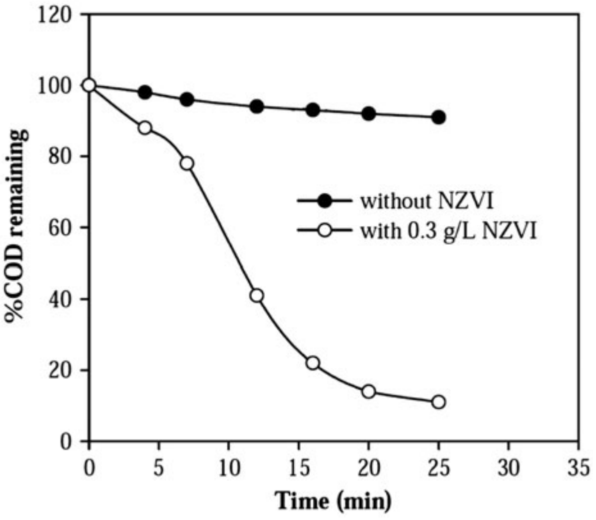

Fig. 6. Effect of sonication time on% COD remaining. Experimental conditions: EBBR, 100 ppm, pH = 3, NZVI, and 0.3 g/L.

4. Conclusion

In this study nano-size zero-valent iron particles have been synthesized through a liquid-phase reduction method and used for decolorization of EBBR dye in combination of ultrasonic irradiation. The results indicate that ultrasonic irradiation can accelerate the reduction of organic dye molecules with NZVI particles. Batch experiments have been used to obtain the best parameters for getting maximum removal of color. The degradation of EBBR in aqueous solutions with NZVI under ultrasonic irradiation followed the pseudo-first-order reaction kinetics. The removal percent of color was found to be decreased with increase in initial pH and increase with decrease in the initial concentration of the solution. Decolorization kinetic rate constants obtained by pseudo-first-order rate equation increased 0.46 min^{-1} per increase of 1 g/L of NZVI concentration and 0.15 min^{-1} per increase of 1% w/v of NaCl.

Acknowledgment

The authors wish to express their gratitude to the Shahid Beheshti University of Medical Sciences Research Council for the support of this work.

References

[1] Kirk-Othmer, Encyclopedia of Chemical Technology, fourth ed., Vol. 3, John Wiley, New York, NY, 1998.

[2] K.T. Chung, C.E. Cerniglia, Mutagenicity azo dyes: Structure activity relationships, Mutat. Res. 277 (1992) 201–220.

[3] W. Zhang, H. Yang, L. Dong, H. Yan, H. Li, Z. Jiang, X. Kan, A. Li, R. Cheng, Efficient removal of both cationic and anionic dyes from aqueous solutions using a novel amphoteric straw-based adsorbent, Carbohydr. Polym. 90 (2012) 887–893.

[4] J. Labanda, J. Sabaté, J.L. lorena, Experimental and modeling study of the adsorption of single and binary dye solutions with an ion-exchange membrane adsorber, Chem. Eng. J. 166 (2011) 536–543.

[5] L.C. Almeida, S. Garcia-Segura, C. Arias, N. Bocchi, E. Brill, Electrochemical mineralization of the azo dye Acid Red 29 (Chromotrope 2R) by photoelectro-Fenton process, Chemosphere 89 (2012) 751–758.

[6] M. Chafi, B. Gourich, A.H. Essadki, C. Vial, A. Fabregat, Comparison of electrocoagulation using iron and aluminium electrodes with chemical coagulation for the removal of a highly soluble acid dye, Desalination 281 (2011) 285–292.

[7] M. Gao, Z. Zeng, B. Sun, H. Zou, J. Chen, L. Shao, Ozonation of azo dye Acid Red 14 in a microporous tube-in-tube microchannel reactor: Decolorization and mechanism, Chemosphere 89 (2012) 190–197.

[8] K. Turhan, I. Durukan, S.A. Ozturkcan, Z. Turgut, Decolorization of textile basic dye in aqueous solution by ozone, Dyes Pigm. 92 (2012) 897–901.

[9] Y. Qu, X. Cao, Q. Ma, S. Shi, L. Tan, X. Li, H. Zhou, X. Zhang, J. Zhou, Aerobic decolorization and degradation of Acid Red B by a newly isolated Pichia sp. TCL, J. Hazard. Mater. 223–224 (2012) 31–38.

[10] M.A. Rauf, S.S. Ashraf, Survey of recent trends in biochemically assisted degradation of dyes Review Article, Chem. Eng. J. 209 (2012) 520–530.

[11] N.M. Zhu, L. Yi, F.S. Zhang, Catalytic dechlorination of polychlorinated biphenyls in subcritical water by Ni/Fe nanoparticles, Chem. Eng. J. 171 (2011) 919–925.

[12] R.J. Barnes, O. Riba, M.N. Gardner, T.B. Scott, S.A. Jackman, I.P. Thompson, Optimization of nano-scale nickel/iron particles for the reduction of high concentration chlorinated aliphatic hydrocarbon solutions, Chemosphere 79 (2010) 448–454.

[13] T.B. Scott, A.C. Popescu, R.A. Crane, C. Noubactep, Nanoscale metallic iron for the treatment of solutions containing multiple inorganic contaminants, J. Hazard. Mater. 186 (2011) 280–287.

[14] Y. Xi, M. Mallavarapu, R. Naidu, Reduction and adsorption of Pb^{2+} in aqueous solution by nano-zero-valent iron—A SEM TEM and XPS study, Mater. Res. Bull. 45 (2010) 1361–1367.

[15] Y.H. Hwang, D.G. Kim, H.S. Shin, Mechanism study of nitrate reduction by nano zero valent iron, J. Hazard. Mater. 185 (2011) 1513–1521.

[16] S.M. Hosseini, B. Ataie-Ashtiani, M. Kholghi, Nitrate reduction by nano-Fe/Cu particles in packed column, Desalination 276 (2011) 214–221.

[17] H.Y. Shu, M.C. Chang, C.C. Chen, P.E. Chen, Using resin supported nano zero-valent iron particles for decoloration of Acid Blue 113 azo dye solution, J. Hazard. Mater. 184 (2010) 499–505.

[18] T. Satapanajaru, C. Chompuchan, P. Suntornchot, P. Pengthamkeerati, Enhancing decolorization of Reactive Black 5 and Reactive Red 198 during nano zerovalent iron treatment, Desalination 266 (2011) 218–230.

[19] M. Huang, K. Zhao, M. Zhang, S. Chen, W. Xu, Y. Ye, W. Fu, Y. Wei, Z. Qiu, F. Sun, Removal of Disperse Dyes from Wastewater by Nano-iron Modified Goldmine Waste-solid Assisted AOPs, Procedia Eng. 18 (2011) 358–362.

[20] K.R. Kim, B.T. Lee, K.W. Kim, Arsenic stabilization in mine tailings using nano-sized magnetite and zero valent iron with the enhancement of mobility by surface coating, J. Geochem. Explor. 113 (2012) 124–129.

[21] Y.T.g. Lin, C.H. Weng, F.Y. Chen, Effective removal of AB24 dye by nano/micro-size zero-valent iron, Sep. Purif. Technol. 64 (2008) 26–30.

[22] C.P. Chu, B.V. Chang, G.S. Liao, D.S. Jean, D.J. Lee, Observations on changes in ultrasonically treated waste-activated sludge, Water Res. 35 (2001) 1038–1046.

[23] J.M. Joseps, H. Destaillasts, H.M. Hung, M.R. Hoffmann, The sonochemical degradation of azobenzene and related azo dyes: Rate enhancements via fenton's reactions, J. Phys. Chem. A 104 (2000) 301–307.

[24] Y. Zhang, Y. Li, J. Li, L. Hu, X. Zheng, Enhanced removal of nitrate by a novel composite: Nanoscale zero valent iron supported on pillared clay, Chem. Eng. J. 171 (2011) 526–531.

[25] APHA, AWWA and WEF, Standard methods for the examination of water and wastwater, nineteenth ed., American Public Health Association, Washington, DC, 1995.

[26] A. Zille, B. Górnacka, A. Rehorek, A. Cavaco-Paulo, Degradation of azo dyes by trametes villosa Laccase over long periods of oxidative conditions, Appl. Environ. Microbiol. (2005) 6711–6718.

[27] J. Lee, J. Kim, W. Choi, Oxidation on zerovalent iron promoted by polyoxometalate as an electron shuttle, Environ. Sci. Technol. 41 (2007) 3335–3340.

[28] Q.J. Rasheed, K. Pandian, K.T. Muthukumar, Treatment of petroleum refinery wastewater by ultrasound-dispersed nanoscale zero-valent iron particles, Ultrason. Sonochem. 18 (2011) 1138–1142.

[29] Y.H. Lio, S.L. Loa, C.J. Lin, W.H. Kuan, S. CWeng, Chemical reduction of an unbuffered nitrate solution using catalyzed and uncatalyzed nanoscale iron particles, J. Hazard. Mater. 127 (2005) 102–110.

[30] H. Song, E.R. Carrway, Reduction of chlorinated ethanes by nanosized zero-valent iron: Kinetics, pathways, and effects of reaction condition, Environ. Sci. Technol. 39 (2005) 6237–6245.

[31] S. Chatterjee, S.R. Lim, S.H. Woo, Removal of Reactive Black 5 by zero-valent iron modified with various surfactants, Chem. Eng. J. 160 (2010) 27–32.

[32] J. Wang, Z. Jiang, Z. Zhang, Y. Xie, X. Wang, Z. Xing, R. Xu, X. Zhang, Sonocatalytic degradation of acid red B and rhodamine B catalyzed by nano-sized ZnO powder under ultrasonic irradiation, Ultrason. Sonochem. 15 (2008) 768–774.

[33] A. Agrawal, P.G. Tranyek, Reduction of nitro aromatic compounds by zero-valent iron metal, Environ. Sci. Technol. 30 (1996) 153–160.

[34] M. Goel, H. Hongqiang, A.S. Mujumdar, M.B. Ray, Sonochemical decomposition of volatile and non-volatile organic compounds—a comparative study, Water Res. 38 (2004) 4247–4261.

[35] T.M. Elmorsi, Y.M. Riayd, Z.H. Mohamed, M.H.A.E. Bary, Decolorization of Mordant red 73 azo dye in water using H_2O_2/UV and photo-Fenton treatment, J. Hazard. Mater. 174 (2010) 352–358.